Potential Vorticity Analysis of Tropical Cyclone Intensification

JOHN MOLINARI, STEVEN SKUBIS, DAVID VOLLARO, AND FRANK ALSHEIMER

Department of Earth and Atmospheric Sciences, The University at Albany, State University of New York, Albany, New York

HUGH E. WILLOUGHBY

Hurricane Research Division, AOML/NOAA, Miami, Florida

(Manuscript received 14 June 1996, in final form 12 December 1997)

ABSTRACT

The interaction of marginal Tropical Storm Danny (1985) with an upper-tropospheric positive potential vorticity anomaly was examined. The intensification mechanism proposed earlier for mature Hurricane Elena appears to be valid for Danny as well, despite significant differences in the synoptic-scale environment and in the stage of the tropical cyclone prior to the interaction. Both storms experienced rapid pressure falls as a relatively small-scale positive upper potential vorticity anomaly began to superpose with the low-level tropical cyclone center.

The interaction is described in terms of a complex interplay between vertical wind shear, diabatic heating, and mutual advection among vortices at and below the level of the outflow anticyclone. Despite this complexity, the superposition principle appears to be conceptually useful to describe the intensification of tropical cyclones during such interactions.

1. Introduction

Considerable disagreement exists in both the operational and research communities as to whether the approach of an upper-tropospheric, synoptic-scale trough will produce intensification or decay of a tropical cyclone. Although this question might seem easy to resolve empirically, the reality is complex: in addition to containing a positive vorticity anomaly, the upper troughs also can induce increased vertical wind shear over the tropical cyclone as they approach. Observational (Gray 1968; McBride and Zehr 1981) and statistical (DeMaria and Kaplan 1994; DeMaria 1996) studies show that the tropical storm intensification rate tends to vary inversely with the magnitude of vertical wind shear. In support of this view, the structure of tropical cyclones on satellite images frequently becomes disrupted and the storms weaken as upper-tropospheric troughs approach. Conversely, observational studies (Miller 1958; Sadler 1976; Molinari and Vollaro 1990; Davidson et al. 1990; Bosart and Bartlo 1991; Rodgers et al. 1991; DeMaria et al. 1993; see also overviews by Molinari and Vollaro 1989 and Riehl 1979), idealized numerical studies (Holland and Merrill 1984; Pfeffer and Challa 1981, 1992; Montgomery and Farrell 1993), and prior practice among forecasters (Simpson 1971) support the idea that tropical cyclones often intensify during interactions with upper-tropospheric vorticity maxima.

It will be argued, following Hoskins et al. (1985), McIntyre (1993), and many others, that Ertel potential vorticity (hereafter PV) provides a useful dynamical framework for examining such interactions. The same dynamics can, of course, be described by more traditional variables such as vorticity, height, and wind. The added benefit of PV lies in its quasi-conservation properties, analogous to using potential temperature rather than temperature, or θ_e rather than specific humidity. In each case, the preferred variable is conserved under certain specified conditions and thus acts as a tracer on the flow. Unlike absolute vorticity, PV is conserved for frictionless, adiabatic motions. In addition, the PV conservation equation directly ties together the dynamics and the heating, unlike the vorticity equation, which must do so indirectly via the divergence and twisting terms. Potential vorticity is not a panacea, but we believe it provides a more concise framework for interpretation of the observations than the alternatives.

The work of Thorpe (1986; see also Fig. 15 of Hoskins et al. 1985) is relevant to the discussion. Thorpe computed the tangential wind and temperature perturbations associated with a balanced, isolated, circular, upper-tropospheric positive PV anomaly. Vertical shear of the tangential wind increases from zero directly under the PV anomaly to large values outside the core of the anomaly. If a small ambient vertical shear were added

Corresponding author address: John Molinari, Department of Earth and Atmospheric Science, The University at Albany, State University of New York, Albany, NY 12222.
E-mail: molinari@atmos.albany.edu

to Thorpe's diagram, sufficient to move a tropical cyclone toward the PV anomaly, the tropical cyclone would experience a deep layer of vertical wind shear for an extended period (for Thorpe's anomaly, this period would be about 40 h for a tropical cyclone moving at 5 m s^{-1}). If the upper PV anomaly did not change in size or shape, the tropical cyclone would almost certainly be dramatically weakened by the interaction. It is the opposing influence of vertical shear and positive vorticity advection aloft that complicates the problem.

Molinari et al. (1995) examined the potential vorticity evolution during reintensification of Hurricane Elena (1985) in the Gulf of Mexico. A synoptic-scale trough approaching the hurricane experienced distortion similar to that described by Thorncroft et al. (1993) as ''equatorward wave breaking.'' In particular, the later stages of the process resembled blocking-high-induced wave breaking (Thorncroft et al. 1993, 34), with the outflow anticyclone of the hurricane playing the role of the blocking high. As a result of this interaction, a narrow upper-tropospheric positive PV anomaly extending from the original trough eventually became partly superposed over the hurricane core. Intensification of the storm was attributed to the combination of two processes: (i) a ''constructive interference'' between the upper PV anomaly and the lower PV anomaly of like sign associated with the tropical cyclone, in which perturbation energy grows at the expense of the mean vertical wind shear (K. A. Emanuel 1988, personal communication; Hoskins 1990, 68–69; Montgomery and Farrell 1993); and (ii) excitation of an evaporation–wind feedback (''WISHE mode''; Emanuel 1986; Rotunno and Emanuel 1987) by the enhanced surface circulation associated with the upper anomaly. Furthermore, the evidence suggested that enhanced heating associated with the above process eroded the upper PV anomaly and prevented it from crossing the tropical cyclone and reversing the intensification.

A key element of the above evolution was the thinning of the approaching positive PV anomaly. By the reasoning from Thorpe's diagram described above, this process allowed the upper anomaly to approach and partially superpose over the hurricane without producing a long-lasting, deep layer of large vertical shear. The intensification of the tropical cyclone thus did not represent simply the bringing together of two positive PV anomalies. Rather, the upper positive anomaly first had to be reduced in scale by interaction with the outflow anticyclone, which itself was strongly reinforced by low PV provided by convection at the storm core. Molinari et al. (1995) argued that such outflow layer interactions are a fruitful area for further research into tropical cyclone intensity change.

The tropical cyclone in the above study was hurricane strength before the interaction. It was unclear whether weaker tropical disturbances could intensify in a similar manner. In the current study, Hurricane Danny (1985) will be examined during its interaction with an upper positive PV anomaly. Unlike Hurricane Elena, Danny was a disorganized tropical storm before the interaction. In addition, the upper PV anomaly in this study was not associated with a mobile synoptic-scale trough, but was quasi-stationary and subsynoptic scale, and the tropical cyclone approached it rather than the other way around. The goal is to understand the behavior of a weaker storm interacting with a smaller-scale upper PV anomaly and to investigate the roles of vertical wind shear and diabatic heating in the observed evolution.

2. Data and analysis methods

All calculations will be made using gridded analyses from the European Centre for Medium-Range Weather Forecasts (ECMWF). These are uninitialized and contain 12 vertical pressure levels (1000–50 mb) and 1.125° latitude–longitude horizontal resolution. The benefits and limits of ECMWF analyses of tropical cyclones have been extensively discussed by Molinari and Vollaro (1990) and Molinari et al. (1992, 1995).

Hydrostatic Ertel potential vorticity is given by

$$\Pi = g\sigma^{-1}(\zeta_\theta + f),$$

where $\sigma = -\partial p/\partial\theta$ is pseudodensity. Detailed horizontal structure of PV near the storm core cannot be resolved by the ECMWF analyses. Rather, this paper will focus upon larger-scale structures in the hurricane surroundings. Molinari et al. (1995) showed that PV fields in Hurricane Elena (1985) in the Gulf of Mexico exhibited remarkable coherence in time and space as an upper PV maximum became partially superposed over the hurricane. The smooth variation in time of PV does not guarantee accuracy, but at the very least it indicates that the analyses are defining a consistent scale feature that does not, for instance, appear and disappear with the availability of data. Similarly consistent analyses will be shown in the current paper. This analysis skill arises in part because both storms were downstream of regions with extensive rawinsonde coverage. In addition, the four-dimensional analysis and data assimilation procedure used by ECWMF, in which model forecasts are used as first-guess fields, appears to be quite successful in extending accurate analyses into regions with sparse data.

Eliassen–Palm (hereafter E–P) fluxes will also be presented. Willoughby (1978) and Schubert (1985) have developed formulations of E–P fluxes in cylindrical coordinates. The current formulation follows Molinari et al. (1995) and represents a cylindrical analog to the spherical coordinate system of Tung (1986). It includes a relationship between E–P flux convergence and eddy PV flux. Of necessity for tropical cyclone studies, the equations are developed in a storm-following coordinate. Molinari et al. (1995) give the full equations containing diabatic heating, friction, and the spatial variation of f. All calculations in this paper will be carried out on an adiabatic frictionless f plane. The resulting

equation for the time change of azimuthally averaged relative angular momentum per unit volume is given by

$$(r\overline{\sigma v_L})_{t_L} + r^{-1}(r^2(\overline{\sigma u_L})\overline{v}_L)_r + (r\overline{\sigma u})f = \nabla\cdot\mathbf{F}_L. \quad (1)$$

The subscript L indicates storm relative; all other subscripts represent derivatives. The subscript t_L indicates a time derivative following the moving storm; u and v represent radial and tangential velocity, respectively; ∇ is a two-dimensional (r–θ) derivative operator; and the E–P flux vector is given by

$$\mathbf{F}_L \equiv [-r\overline{(\sigma u_L)'v_L'}, \overline{p'\Psi_\lambda'}], \quad (2)$$

where Ψ is Montgomery potential and primes indicate deviations from the azimuthal average. The E–P flux vector $\mathbf{F}_L$ can be interpreted as an ''effective (angular) momentum flux'' (Plumb 1983). It incorporates the impact of both eddy angular momentum fluxes and eddy heat fluxes. The cylindrical coordinate form for E–P flux differs from that commonly used (e.g., Edmon et al. 1980) in that the mean is not a zonal mean but an azimuthal mean that includes the symmetric part of the hurricane. The eddies represent any deviation from the azimuthal mean, including, of course, the upper-tropospheric PV anomalies. When $\nabla\cdot\mathbf{F}_L > 0$, there is a positive eddy-induced torque in the layer. Further details of the E–P flux formulation are given by Molinari et al. (1995).

The E–P flux formulation in the cylindrical coordinate would be most insightful if the azimuthal eddies of interest represented small-amplitude waves propagating azimuthally on the radial PV gradient of the hurricane. These circumstances would make the E–P flux interpretation analogous to that for the global circulation (see, e.g., Edmon et al. 1980). The cylindrical formulation might thus be of greatest value in interpreting high-resolution model output in the tropical cyclone core, where azimuthally propagating waves may play a significant role in connecting core dynamics and larger-scale features (Willoughby 1978; Holland 1987; Guinn and Schubert 1993; Montgomery and Kallenbach 1997). In this study, however, as well as in the previous study of Hurricane Elena, waves on the hurricane's own radial PV gradient cannot be meaningfully resolved and may or may not exist.

Nevertheless, it will be shown that resolvable azimuthal eddies do develop outside the hurricane core at upper levels. The Eliassen–Palm flux convergence will provide a measure of the integrated influence of fluxes by these organized eddies on the azimuthal mean flow. In addition, the vertical variation of $\nabla\cdot\mathbf{F}_L$ will give some insight into the importance of processes at the tropopause during intensification of the tropical cyclone.

Molinari et al. (1995) show that for frictionless adiabatic flow on an f plane, the E–P flux divergence is related to the azimuthal eddy PV flux by

$$-\frac{r\overline{\sigma}^2}{g}\langle u_L^*\Pi_L^*\rangle = \nabla\cdot\mathbf{F}_L - (r\overline{\sigma' v_L'})_{t_L}, \quad (3)$$

where the angle brackets and asterisk indicate pseudo-density-weighted azimuthal mean and deviation, respectively. Molinari et al. (1995) also showed that within 1000 km of the center the E–P flux divergence closely resembles the eddy PV flux term in (3).

3. Inner core evolution

Figure 1 shows the azimuthal mean tangential velocity during two aircraft reconnaissance flights into Tropical Storm Danny (Willoughby 1990). Also shown is the rate of change of velocity (m s^{-1} per 6 h) during the flight. The analysis and interpolation methods used to obtain these plots are identical to those given by Willoughby (1990), but the algorithms have been applied separately to each flight rather than for the two flights combined.

Figure 1a shows that Danny was a marginal tropical storm with a broad, flat tangential wind profile between 1500 and 2100 UTC 14 August. The maximum tangential velocity of about 20 m s^{-1} occurred 130 km from the center. Tangential velocity increased with time during this flight over a broad radial region from the 30-km radius to beyond the 150-km radius. About 15 h later (Fig. 1b), the tangential velocity profile had dramatically changed. An eyewall profile was present, with a nearly linear increase of mean tangential velocity with radius to more than 30 m s^{-1} at $r = 70$ km. Reconnaissance aircraft found winds locally exceeding 34 m s^{-1}, indicating that the storm had reached hurricane intensity. The time change of tangential velocity showed a signature characteristic of a contracting eyewall (Willoughby 1990; Willoughby et al. 1982). In subsequent hours the storm rapidly intensified as this contraction occurred. The process was cut short by landfall at 1740 UTC 15 August. Sea surface temperatures averaged over the week prior to the passage of Hurricane Danny (produced by Reynolds and Smith 1994) were 0.4°–0.5°C warmer than the long-term mean near the Gulf Coast, but were virtually constant along the storm path during the last 12 h before landfall. Because Tropical Storm Danny changed dramatically in structure during this time, it appears that other factors must be playing a role. One of the goals of this paper is to describe the evolution of the larger-scale environment of Hurricane Danny and its possible relation to the rapid development of the eyewall shown in Fig. 1.

4. Larger-scale evolution

a. Upper-tropospheric PV

Figure 2 shows PV at the 350-K potential temperature level for six observation times 12 h apart, starting from about 36 h before and ending 24 h after eyewall formation. Following Molinari et al. (1995), the 350-K level was chosen for display because it contained the largest Eliassen–Palm flux divergence (and the largest

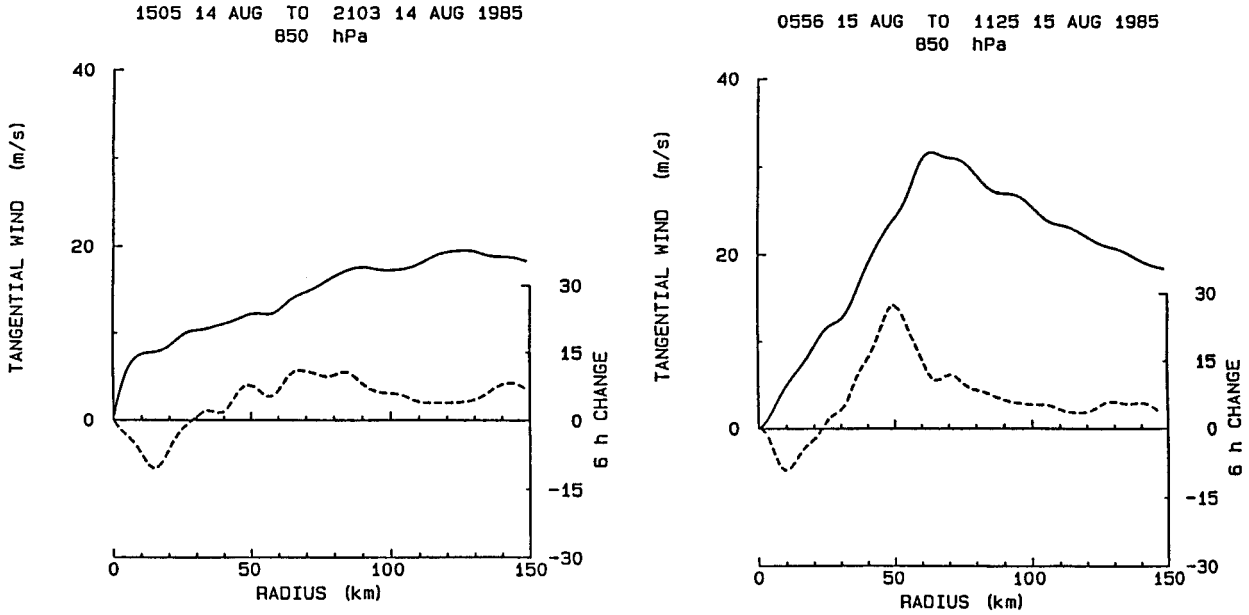

FIG. 1. Azimuthal mean 850-mb tangential wind profile (solid; m s^{-1}, left axis) and its six-hourly time change (dashed, m s^{-1} per 6 h, right axis) from reconnaissance aircraft data for two flights into Hurricane Danny. Based on the analysis method of Willoughby (1990).

azimuthal eddy flux of PV) at the time the eyewall developed. The 350-K level lies between 175 and 225 mb in the region shown in Fig. 2.

In the upper troposphere well outside the hurricane core, where diabatic and frictional sources and sinks should be small, PV must be nearly constant following air parcels, and thus PV maxima and minima should be preserved on an isentropic surface. It is notable in Fig. 2 that the magnitudes of PV in local maxima relatively far from the hurricane do indeed remain nearly constant throughout the 60-h period. This provides some confirmation of the quasi-conservative behavior of PV in the ECMWF analyses.

The term PV ''anomaly'' will often be used in this paper, although no explicit reference state will be defined. Following the reasoning of Hoskins et al. (1985, 897), ''anomaly'' will implicitly refer to a deviation from an area average on an isentropic surface. Because well-defined maxima and minima appear in the fields shown in Fig. 2, substitution of the term ''positive (or negative) anomaly'' for ''local PV maximum (minimum)'' is appropriate. Potential vorticity will be expressed in the units of Hoskins et al. (1985) (1 PVU = 1×10^{-6} m^2 K s^{-1} kg^{-1}).

At the initial time (1200 UTC 13 August, Fig. 2a), the outflow anticyclone was nearly centered over the surface position of the tropical storm. A PV maximum existed 1200 km northwest of the tropical storm center. Both the PV maximum and the tropical storm had moved northwestward over the previous 24 h, so that the distance between them had changed little. A larger-scale trough was slowly moving eastward from the northwest corner of the region. Over the next 12 h, the PV maximum over Louisiana stopped moving westward and turned slowly toward the north, apparently due to the wind from the south at its center associated with the outflow anticyclone. The reduction in westward motion of the PV maximum allowed the tropical cyclone to approach it.

At 0000 UTC 14 August (Fig. 2b), the strong, well-defined outflow anticyclone remained centered over the tropical storm. The positive PV anomaly over Louisiana had become considerably distorted as a result of the greatly enhanced northward flow of low-PV air from the tropical storm. As noted by Molinari et al. (1995), such distortion can be interpreted as an interaction on the 350-K surface between a strong negative PV anomaly (the outflow anticyclone) and the positive anomaly in the environment. The PV gradient between the two features strengthened from the earlier time.

By 1200 UTC 14 August (Fig. 2c), the interaction had continued, and both PV anomalies had become further deformed. The tropical cyclone moved away from the center of the outflow anticyclone and was approaching the strong PV gradient on its western edge. This process continued over the following 12 h, and by 0000 UTC 15 August (Fig. 2d), the tropical storm had moved under the large PV gradient. It was near this time that the eyewall formed in the storm. The area of near-zero PV air expanded, especially north of the tropical cyclone, and the positive PV anomaly to the northwest was further distorted. By 1200 UTC 15 August (Fig. 2e), low PV air had extended farther north and west, and the original PV maximum had essentially been split into two. By 0000 UTC 16 August (Fig. 2f), only a

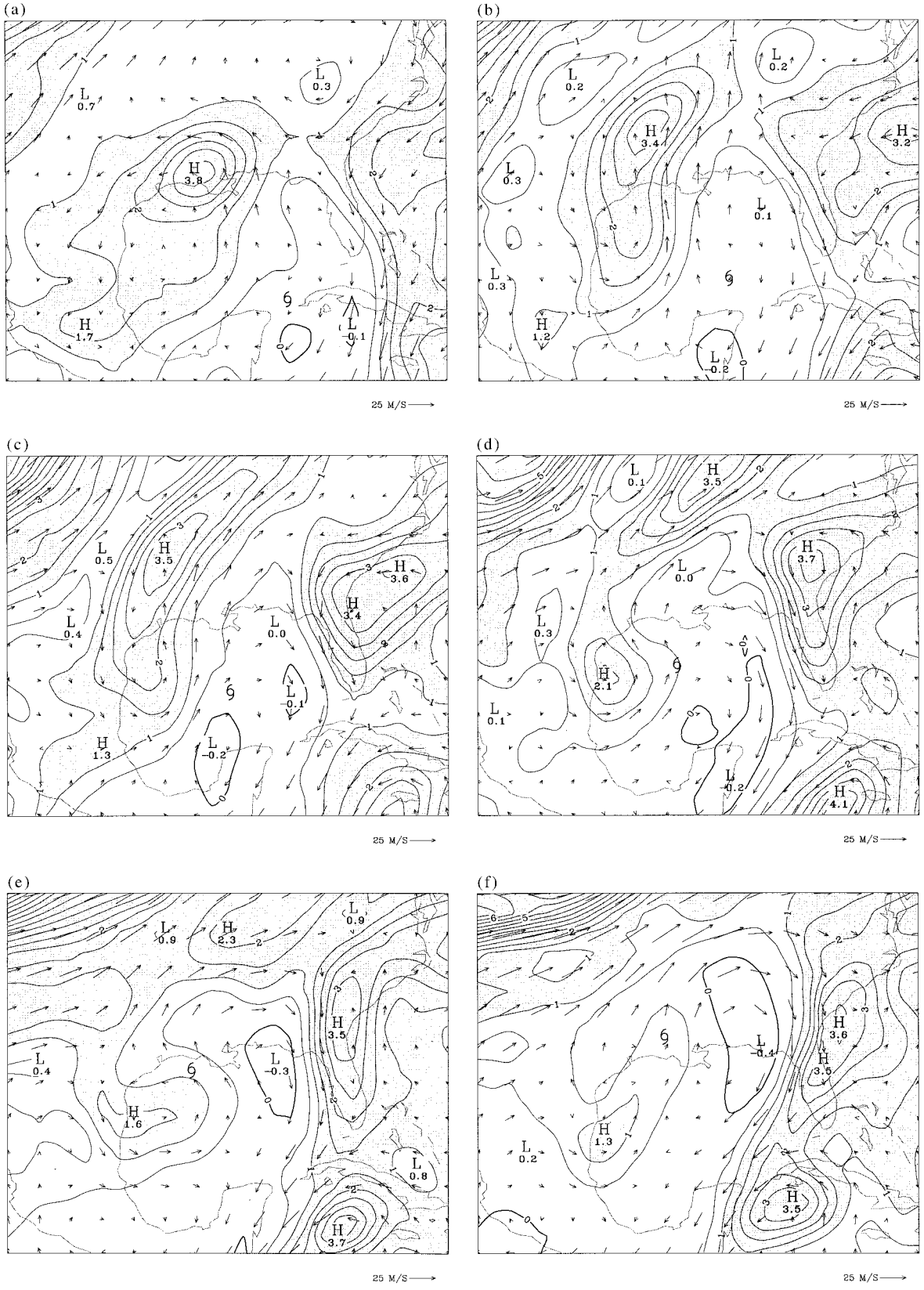
(a)
L 0.7
L 0.3
H 3.8
H -1.7
L -0.1
25 M/S
(b)
L 0.2
L 0.2
H 3.4
H 3.2
L 0.3
L 0.1
L 0.3
H 1.2
L -0.2
25 M/S
(c)
L 0.5
H 3.5
H 3.6
H 3.4
L 0.4
L 0.0
L -0.1
H 1.3
L -0.2
25 M/S
(d)
L 0.1
H 3.5
H 3.7
L 0.0
L 0.3
H 2.1
L 0.1
L -0.2
H 4.1
25 M/S
(e)
L 0.9
H 2.3
L 0.9
H 3.5
L 0.4
L -0.3
H 1.6
L 0.8
H 3.7
25 M/S
(f)
L -0.4
H 3.6
H 3.5
H 1.3
L 0.2
H 3.5
25 M/S

small region of greater than 1 PVU remained, and low PV wrapped around to the southwest of the center.

The observed PV evolution supports the contention by Molinari et al. (1995) that tropical cyclone interactions with upper PV anomalies do not represent simply the bringing together of positive anomalies, but rather that interaction with the tropical cyclone's outflow anticyclone initially plays a major role. The interaction will be quantified in terms of Eliassen–Palm flux convergences in the following section.

b. Eliassen–Palm fluxes

The cross sections of E–P flux vectors (not shown) contained maximum divergence (and thus largest angular momentum spinup) in a narrow layer around 350 K throughout the period. The region of $\nabla \cdot \mathbf{F}_L > 0$ was smaller in radial extent than in Hurricane Elena (Molinari et al. 1995), consistent with the smaller lateral extent of the upper PV anomaly.

Figure 3 shows a radius–time series of $(r\overline{\sigma})^{-1}\nabla \cdot \mathbf{F}_L$ on the 340-K and 350-K surfaces. This quantity represents the influence of eddy activity on mean tangential velocity (Molinari et al. 1995) and is expressed in units of m s^{-1} day^{-1}. As noted earlier, it is also a good representation of tangential velocity change as a result of PV flux by azimuthal eddies. At 340 K (Fig. 3a) the steady approach of the tropical storm toward the trough can be seen, and spinup by eddy PV flux reached a maximum at the 600-km radius at 1200 UTC 14 August, then decreased thereafter. The time variation of the same field at 350 K (Fig. 3b) was strikingly different. A rapid increase in the tangential wind speed occurred at the 500-km radius on 0000 UTC 15 August, the approximate time of eyewall development.

The reasons for the above behavior can be seen in the relevant PV distributions on each surface. Figure 4 shows PV on 340 K at 0000 UTC 15 August. Except for small regions well removed from the tropical cyclone center, the nominal dynamic tropopause (1.5 PVU) lies entirely above this surface, and PV gradients near the storm are weak. The differences in PV at 350 K are apparent from Fig. 2. In this layer, it was the mutual deforming of strong anomalies, as well as the relative approach of the anomalies, that contributed to the eddy PV flux. In addition, the tropopause intersects this level, dividing the positive PV anomaly (with its low tropopause) from the outflow anticyclone. This geometry ensures a large horizontal gradient of potential vorticity, which is maintained by the supply of low PV air from the tropical cyclone core (Wu and Emanuel 1993; Molinari et al. 1995). As the tropical storm moved under this gradient (Fig. 2d), the storm-relative eddy PV flux and associated tangential velocity spinup became quite large. Molinari et al. (1995) showed similar behavior in Hurricane Elena. Bosart and Lackmann (1995) noted that Hurricane David (1979) intensified over land in part due to lifting of the tropopause by diabatic heating, which created a steeper tropopause (i.e., stronger PV gradient) between the storm and an upstream trough.

In the lower stratosphere above 350 K, a positive PV anomaly eventually moved directly over the low-level center (see Fig. 6f in section 4d). This anomaly was above the level of the outflow layer and its associated anticyclone and was unaffected by the interactions described above. As a result, large eddy activity was present only within a narrow layer where the outflow anticyclone and the upstream positive PV anomaly coexisted. In the following section the processes responsible for the PV evolution within this layer will be examined.

c. Effects of vertical wind shear, diabatic heating, and vortex interactions

As a consequence of the conservation properties of PV, the evolution of the outflow layer PV in Fig. 2 must be the result of conservative (i.e., advective) processes and/or nonconservative processes (see, e.g., Raymond 1992). The major parts of the advective transport are (i) advection of the upper-tropospheric low PV anomaly away from the hurricane in the direction of the vertical shear vector (Shapiro 1992; Wu and Emanuel 1993), (ii) mutual advection between the positive and negative PV anomalies at 350 K, and (iii) mutual advection between 350-K anomalies and anomalies above and below (Jones 1995). Nonconservative processes at this level would occur as a result of (i) transport down the absolute vorticity vector as a result of diabatic heating (e.g., Raymond 1992) and (ii) possibly as a result of vertical eddy transport of heat and momentum by unresolved convection. As an example of the latter, Shapiro (1992) incorporated cumulus momentum sources into his three-layer tropical cyclone model. This influence would be small if unresolved motions were quasi-balanced and thus nearly along surfaces of constant absolute momentum (e.g., Emanuel 1986, 586).

The PV fields in Fig. 2 come from global analyses, and it has proven difficult to calculate meaningful nonconservative terms. Several attempts were made to com-

←

FIG. 2. Wind vectors and Ertel potential vorticity on the 350-K potential temperature surface at (a) 1200 UTC 13 August, (b) 0000 UTC 14 August, (c) 1200 UTC 14 August, (d) 0000 UTC 15 August, (e) 1200 UTC 15 August, and (f) 0000 UTC 16 August 1985. Potential vorticity increment is 0.5×10^{-6} m^2 K s^{-1} kg^{-1} (0.5 PVU), and values greater than 1 PVU are shaded. Wind vectors are plotted each 2¼° latitude–longitude, half their original resolution. The 350-K pressure ranges from 175 to 225 mb, with higher values near or at the tropical cyclone center. The tropical storm symbol indicates the observed position of Tropical Storm/Hurricane Danny.

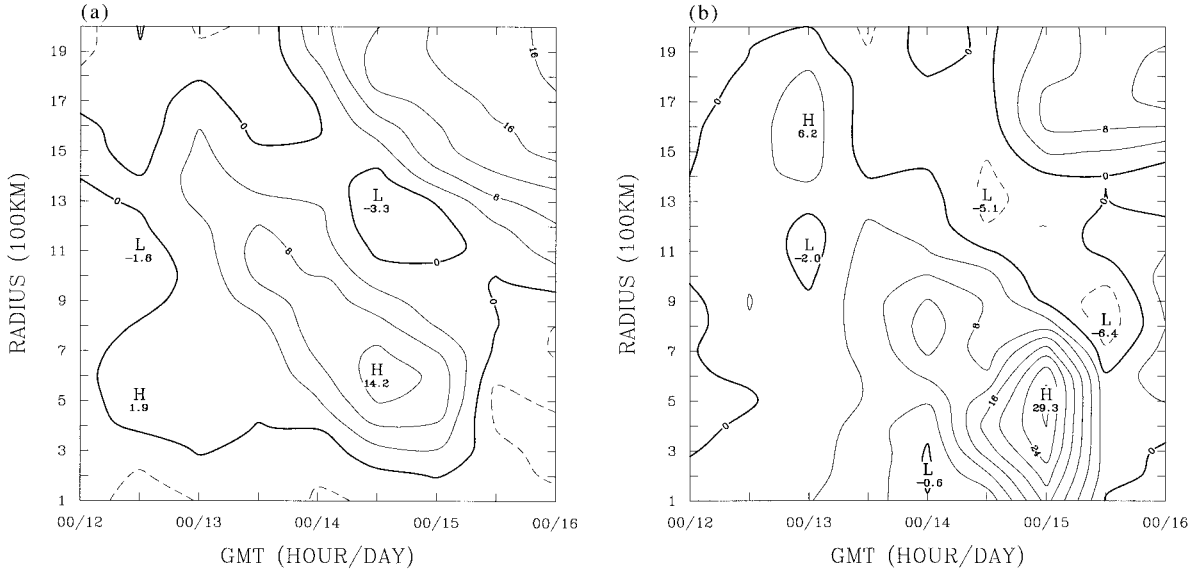

FIG. 3. Radius–time series of the impact of wave activity on the mean tangential velocity, given by $(r\overline{\sigma})^{-1}\nabla\cdot\mathbf{F}_L$, at (a) 340 and (b) 350 K. The plotting increment is 4 m s^{-1} day^{-1}, and negative contours are dashed.

pute diabatic terms as a residual from a PV budget, but with little success. The major problem appeared to arise from truncation errors in the time derivative term due to the 12-h separation of the analyses. A Lagrangian budget following the storm failed to sufficiently reduce these errors. Subgrid-scale sources may also have contributed to the problem. Because part of the advective transport of PV comes from divergent flow associated with the heating, a clear separation of effects might be difficult even with perfect data. Nevertheless, some qualitative comments will be made, based on the effects of vertical wind shear, that provide some evidence for the observed evolution of outflow layer asymmetries.

Vertical wind shear in the layer 850–200 mb was averaged over a radius of 500 km following Molinari (1993). This method of computing the vertical shear removes the azimuthal mean part while retaining the cross-storm component. It is not overly sensitive to the choice of the averaging radius (Molinari 1993). The vertical shear magnitude increased to 11 m s^{-1} on 1200 UTC 14 August as the storm approached the upper anomaly, then fell to 8 m s^{-1} 12 h later, just prior to rapid deepening, and fell to 3 m s^{-1} several hours after rapid deepening. Thus, although vertical shear was decreasing with time, small values of vertical shear followed, rather than preceded, the deepening. In addition, these changes in shear are not externally imposed but, rather, are strongly coupled with the entire interaction process. As a result, vertical shear will be discussed not as an independent cause of deepening or filling, but in concert with changes in other parameters.

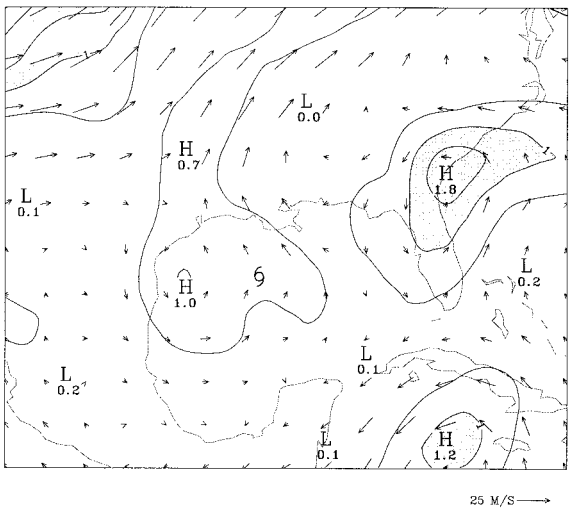

FIG. 4. As in Fig. 2 but on the 340-K potential temperature surface at 0000 UTC 15 August.

Figure 5 shows the vertical variation of the zonal wind, also averaged over the inner 500 km of radius, for 0000 and 1200 UTC 14 August and 0000 UTC 15 August. The 850–200-mb vertical wind shear vector was from the northwest at 0000 UTC 14 August and was within 10 degrees of straight west during the latter two times. As a result essentially all of the deep-layer shear at the last two times is given by the variation of the zonal component in Fig. 5. The strongest vertical shear at these times existed between 300 and 200 mb, equivalent to isentropic levels between 340 and 350 K. At 1200 UTC 15 August and 0000 UTC 16 August, the 850–200-mb vertical wind shear vector (not shown) turned to almost directly from the south and weakened somewhat.

By the reasoning of Shapiro (1992) and Wu and Emanuel (1993), the low PV of the outflow anticyclone

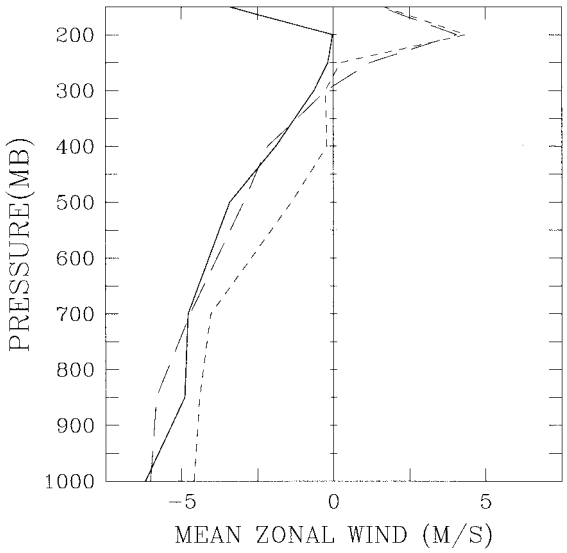

FIG. 5. Vertical variation of the zonal wind velocity, averaged over the inner 500 km of radius, for 0000 UTC 14 August (solid), 1200 UTC 14 August (long dash), and 0000 UTC 15 August (short dash).

should be advected east of the storm (downshear), which indeed occurred by 1200 UTC 14 August. The deep positive PV anomaly associated with the tropical storm should then advect the upper PV anomalies cyclonically (see Jones 1995) thereafter. The observed evolution of PV in Fig. 2 was qualitatively consistent with these interpretations, as low PV appeared north, northwest, and finally west of the tropical cyclone center. One result of this process is the pinching off and scale reduction of the upper positive PV anomaly. This in turn reduces the magnitude and duration of the vertical shear over the storm as it approaches the upper anomaly. Because the evolution of vertical shear is closely tied to the evolution of the upper positive PV anomaly as it interacts with the hurricane, the overall influence of vertical wind shear is quite complex and not easy to untangle.

The observations shown thus far indicate that the interaction between the upper-tropospheric trough and the tropical cyclone involve a coupled evolution of vertical shear, vortex interactions in the horizontal and vertical, and diabatic heating. In the following section, vertical cross sections of PV will be used to suggest that, despite these complexities, superposition is a useful concept to describe the process.

d. Vertical cross sections of PV

Figure 6 displays west–east vertical cross sections of PV at the same times as in Fig. 2. At 1200 UTC 13 August (Fig. 6a), a positive upper PV anomaly in the west–east cross section was present within 1200 km of the center. As Danny approached this anomaly over the next 24 h (Figs. 6b,c), the PV gradient between the two became larger. The PV maximum associated with the tropical cyclone tilted eastward, consistent with the westerly shear shown in Fig. 5. Using the 1.5-PVU surface as the nominal tropopause, it is clear that the upper positive PV maximum is associated with a local lowering of the tropopause.

By 0000 UTC 15 August (Fig. 6d), the 1.5-PVU surface lowered to 355 K over the center, and the 0.5-PVU contours from the upper PV maximum and the hurricane became connected throughout the troposphere. It was at or shortly after this time that the eyewall developed. At 1200 UTC 15 August (Fig. 6e), the upper positive anomaly appeared to erode, but this is partly misleading, because the upper anomaly rotated out of the west–east plane (see Fig. 2e). To the east of the center, the tropopause height sharply increased from its previous values. Central pressure in the hurricane, which had been falling previously by less than 0.5 mb h^{-1}, began to fall more than 1 mb h^{-1} after 0600 UTC 15 August. By 0000 UTC 16 August (Fig. 6f), little evidence of the positive upper anomaly remained, and the PV maximum associated with the hurricane had become almost vertical.

As noted earlier, the role of diabatic heating in this evolution could not be directly calculated. A radar-derived heating rate is probably the most reliable measure of inner core heating. Molinari (1993), using radar-derived estimates of Marks (1985) in Hurricane Allen (1980), showed that diabatic heating within the inner core was largest not when Allen was most intense, but rather when upward motion and outflow calculated from an adiabatic, frictionless nonlinear balance model (Molinari and Vollaro 1990) was strongest. This time coincided with the interaction of Hurricane Allen with an upper positive PV anomaly. Because radar-derived heating is not available for Hurricane Danny, the balanced radial–vertical circulations were calculated to provide an indirect measure of heating forced by larger-scale circulations.

Figure 7 shows a radius–time series of outflow calculated from the balanced model. By far the largest balanced outflow occurred on 0000 UTC 15 August, close to the time when the eyewall developed and the low-level wind structure changed dramatically (Fig. 1). Associated with this was an upper-tropospheric maximum upward motion from the balance model of 8 μbar s^{-1}. On the basis of the Hurricane Allen results (Molinari 1993), diabatic heating would be expected to have significantly increased at this time in Hurricane Danny.

Figure 8 shows storm-relative trajectories on the 350-K isentropic surface for two 12-h periods in Hurricane Danny. The periods are just before and just after the presumed time of largest diabatic heating. Cyclonically curved trajectories and strong cross-storm flow existed during the earlier time. At the latter time, however, the region of upper cyclonic curvature was virtually eliminated in the vicinity of the storm core. The process is reminiscent of the upper-tropospheric evolution in the idealized simulations of Montgomery and Farrell (1993), who also emphasize the importance of low static

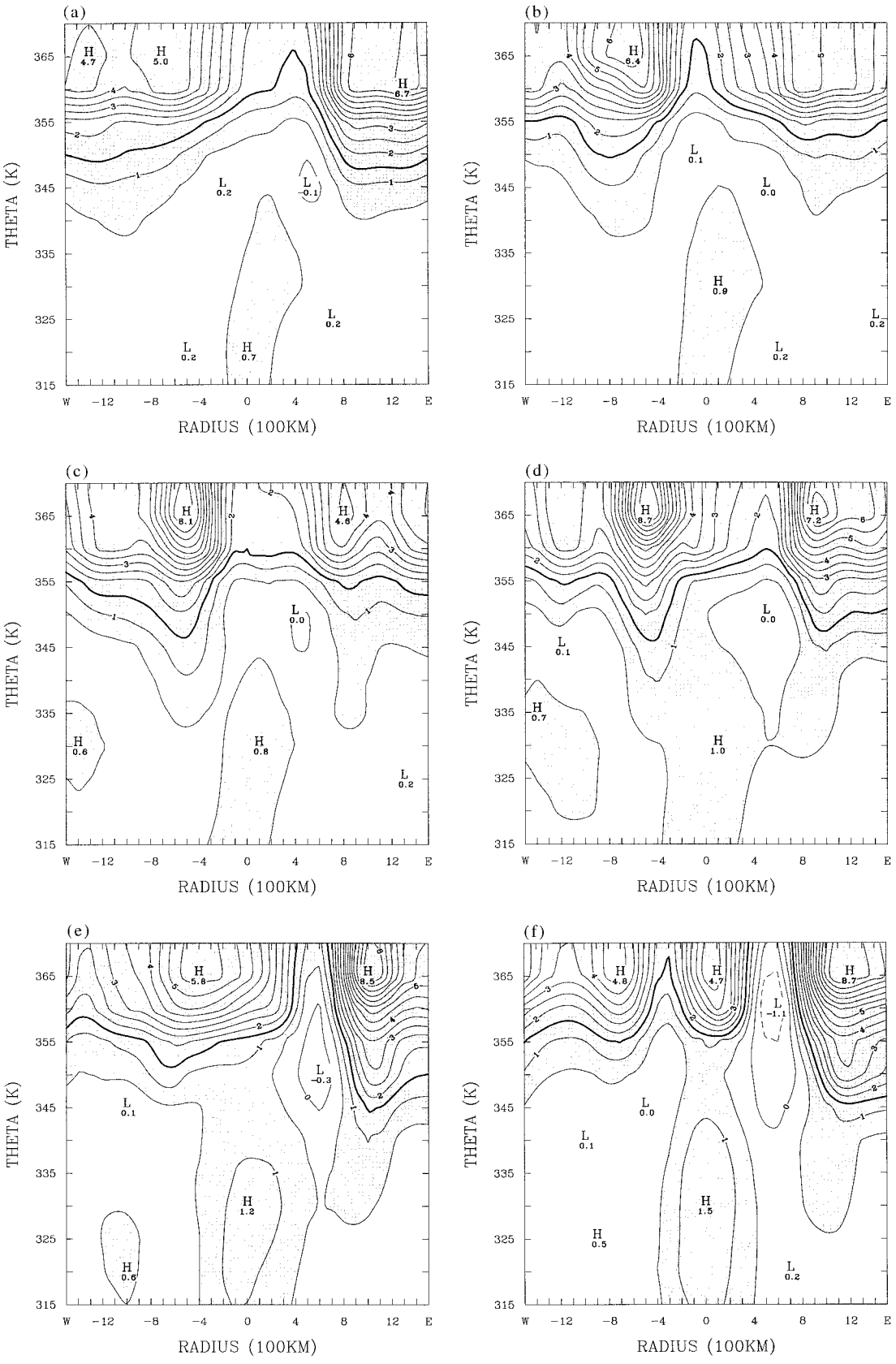
(a)
(b)
(c)
(d)
(e)
(f)
THETA (K)
RADIUS (100KM)
W
E
315
325
335
345
355
365
−12
−8
−4
0
4
8
12

stability in enhancing the response to the trough. The rather sudden change in outflow layer structure in Fig. 8 suggests that significant enhancement of the heating did not occur until the saturated, low-static-stability tropical cyclone core moved under the upper PV anomaly.

Molinari et al. (1995) proposed for Hurricane Elena that enhanced diabatic heating associated with superposition eroded the upper PV anomaly, preventing it from crossing the core and reversing the constructive interference. Figures 7 and 8 provide indirect support for this conjecture in Hurricane Danny. This erosion involves two processes. The first is the loss of PV above the level of maximum heating (Schubert and Alworth 1987). The second process is the outward advection of small PV by the divergent flow associated with the convection (Schubert and Alworth 1987; Möller and Smith 1994). This both slows the approach of the positive PV anomaly toward the center and increases the PV gradient. The large inward eddy PV flux shown in Fig. 3b at the time of the rapid deepening of Hurricane Danny is associated with this process. This indirect evidence suggests that diabatic heating played an essential role during the final stages of the favorable interaction of the upper PV anomaly and the tropical cyclone.

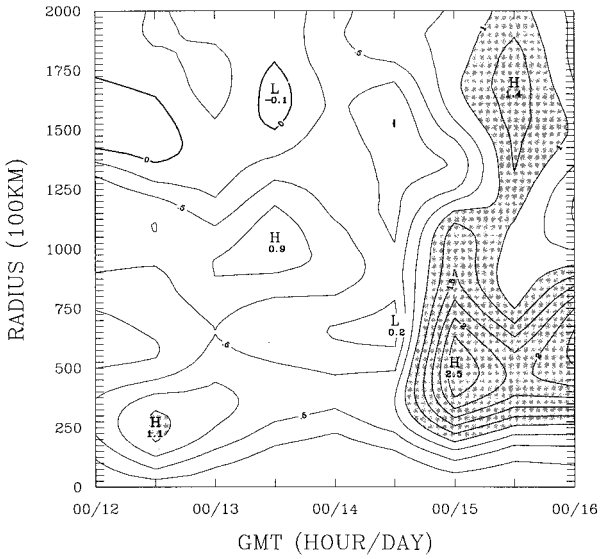

FIG. 7. Radius–time series of 200-mb radial velocity determined from the balanced vortex model of Molinari and Vollaro (1990). Increment: 0.25 m s^{-1}. Values greater than 1 m s^{-1} are shaded, and the zero contour is darkened.

5. Discussion

The superposition principle of potential vorticity has been applied to a second case of interaction between a tropical cyclone and an upper-tropospheric positive potential vorticity anomaly. The final stages of the interaction of disorganized Tropical Storm Danny with a subsynoptic-scale upper PV maximum were similar to those of mature Hurricane Elena (Molinari et al. 1995), despite considerable differences in the synoptic-scale environment. In both storms, rapid deepening began as a small-scale upper-tropospheric PV anomaly became partially superposed over the surface center of the tropical cyclone. In Danny, the initial eyewall formed during the process. As with Hurricane Elena, however, it is uncertain whether the eyewall formation and subsequent contraction was an essential part or simply a consequence of the development.

Recently Emanual (1997) argued that the tropical cyclone can be represented conceptually as a disturbance with zero moist PV in the interior and a large positive θ_e anomaly at the surface. Emanuel noted that if a positive vorticity anomaly on the tropopause of the same scale as the surface entropy source (i.e., the surface circulation) were brought over the tropical cyclone, PV inversion arguments indicate that the tropical cyclone would intensify (see also Thorpe 1985). As noted earlier, the magnitude and duration of vertical wind shear would be small for such an anomaly during its approach and superposition, which also favors intensification. These arguments indicate the importance of scale reduction of the upper-tropospheric positive PV anomaly prior to the superposition.

Such a scale reduction clearly occurred in the Danny case, as is apparent from the evolution of PV in Fig. 2, but it has proven difficult to untangle the process. Vertical wind shear, diabatic heating, and PV anomalies in and below the upper troposphere evolve in a highly coupled sense. Vertical wind shear acted initially to bring the upper and lower positive PV anomalies toward one another. As weak Tropical Storm Danny approached the upper PV anomaly, the upper anomaly became increasingly distorted, as did the outflow anticyclone of the storm. In addition, vertical wind shear began to increase over the storm, and the outflow anticyclone was moved off center. Once the latter occurred, advection of the anticyclone, as well as the positive PV anomaly at the same level, by the cyclonic vortex underneath (Jones 1995) contributed to further distortion and cyclonic rotation of these features with time. As a consequence of these processes, the upper positive PV anomaly was reduced in scale prior to superposition, which in turn weakened the vertical wind shear.

Diabatic heating cannot be determined meaningfully

←

FIG. 6. (a)–(f) West–east (west to the left) cross sections of potential vorticity through the observed center of Hurricane Danny, for the same times as in Fig. 2. Increment: 0.5 PVU. Values greater than 0.5 PVU are shaded, and the nominal tropopause contour (1.5 PVU) is darkened.

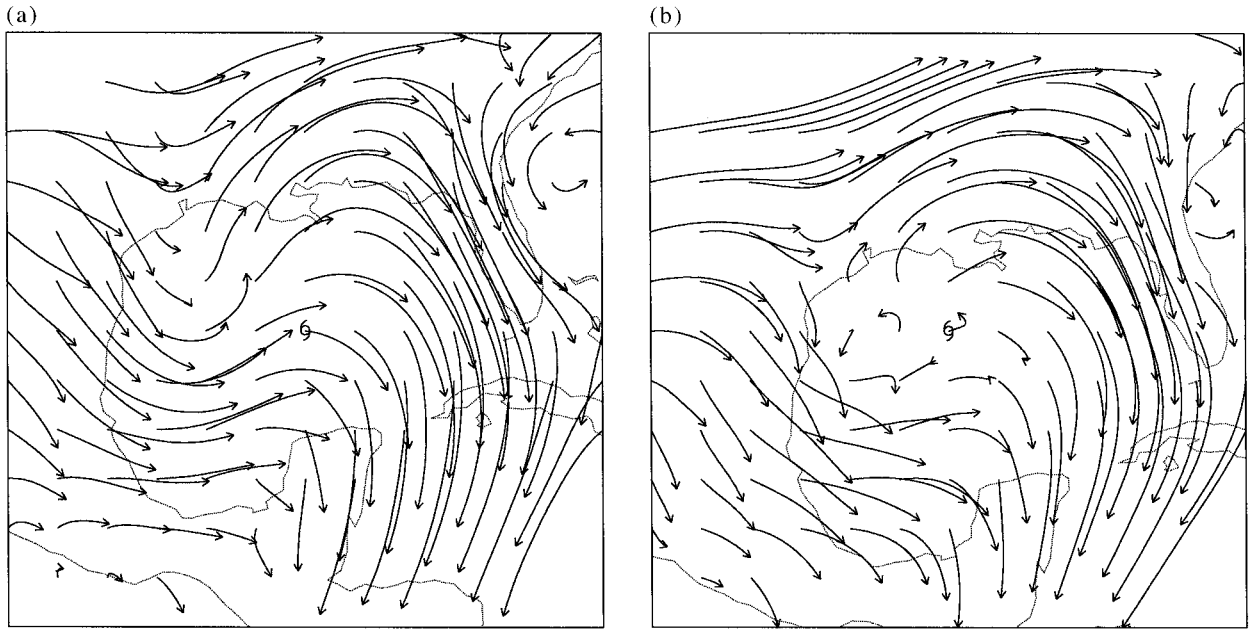

FIG. 8. Storm-relative trajectories on the 350-K isentropic surface: (a) From 1200 UTC 14 August to 0000 UTC 15 August, before the partial superposition of the upper PV anomaly and (b) from 0000 UTC 15 August to 1200 UTC 15 August, subsequent to the superposition. The trajectories originate at grid points, with every other point plotted. Only trajectories that end within the plotted region are shown.

from the global analyses used in this study. Instead, a period of enhanced heating on 15 August was inferred from the sharp increase of adiabatic, dynamically driven radial–vertical circulation associated with the coming together of the tropical cyclone and the upper PV anomaly. The presence of enhanced heating was also supported by dramatic changes in parcel trajectories in the outflow layer during the same period. It is apparent from Figs. 2e and 2f that the area of large positive potential vorticity declined significantly on 15 August, and the upper positive PV anomaly never crossed the center and reversed the intensification. It appears based on the descriptions above that vertical shear, vortex interactions in the horizontal and vertical, and diabatic heating combined to bring about intensification of the tropical cyclone during the interaction with the upper positive PV anomaly.

What happens at the tropical cyclone core during such interactions remains uncertain. Molinari et al. (1995) proposed for Hurricane Elena that as the superposition occurred, a constructive interference process initiated an evaporation–wind feedback instability (''WISHE'' mode; Emanuel 1986). Because few inner core data are available, both the constructive interference and WISHE mechanisms for deepening are speculative at present. It can be said only that the results for Hurricane Danny provide some qualitative support for such an evolution. The constructive interference would enhance the surface circulation and thus create stronger surface fluxes, which could account for the sudden appearance of an eyewall as the added surface moist static energy is distributed vertically by convection. The WISHE mechanism could be responsible for the ensuing intensification of Danny once the stronger surface circulation was initiated. The evidence for an increase in heating after the superposition is not inconsistent with this hypothesis.

Montgomery and Farrell (1993) provide an alternative interpretation of hurricane deepening during trough interactions. In their model, surface spinup resulted from enhanced convergence and vortex stretching in the low static stability inner core. In nature, the enhanced surface fluxes arising from stronger surface winds may evolve simultaneously and in a coupled manner with enhanced vertical circulations and convection induced by the approach of the upper trough. By that reasoning, the question of what comes first, surface fluxes or convection, may not be important. Smith (1997) reached a similar conclusion in his discussion of the theories of CISK (conditional instability of the second kind, as defined by Ooyama 1982) and WISHE (Emanuel 1986; Rotunno and Emanuel 1987). The mechanisms proposed from observations in this paper and from idealized modeling by Montgomery and Farrell (1993) may be different ways of viewing the same process.

The three storms studied by the current authors (Molinari et al. 1995, Molinari 1993, and the present paper) all intensified during superposition of a relatively weak, shallow upper positive PV anomaly. It is well known to operational forecasters, however, that trough interactions can also produce weakening of a storm (Lewis and Jorgensen 1978). Based on the hypotheses presented above, it would be expected that superposition of a deep, large-scale PV anomaly would be unfavorable because vertical shear would occur over a deep layer for a long

period of time and because the induced circulation below would not be on the scale of the tropical cyclone. In such circumstances, the influence of vertical shear would likely dominate that of favorable potential vorticity interactions.

The exact nature of the interactions between the upper positive PV anomaly and the hurricane remains elusive because the tropical cyclone core is inadequately observed. A variety of behaviors can be elicited by the vertical aligning of vortices even in a frictionless, adiabatic, two-layer quasigeostrophic model (Polvani 1991). A great need exists for systematic study of hurricane–trough interactions with a hierarchy of numerical models that isolate the various mechanisms and for observations of the upper troposphere during such interactions.

Acknowledgments. We benefitted from conversations with Dr. David Raymond of New Mexico Tech. We also thank Drs. Roger Smith, Michael Montgomery, and Chris Landsea for their comments and careful reading of the manuscript. Gridded analyses were obtained from the European Centre for Medium-Range Weather Forecasts via the National Center for Atmospheric Research, which is funded by the National Science Foundation. This study was supported by Office for Naval Research Grants N00014-94-I-0289 (JM) and N00014-94-F-0045 (HEW) and by National Science Foundation Grant 9529771.

APPENDIX

Corrigendum to Molinari et al. (1995)

The "L" subscript indicating storm-relative motion was inadvertantly left off some wind component symbols in appendix equations (11) and (13) in the paper by Molinari et al. (1995). These printed errors had no impact on the results of the paper. The correct form of the equations is

$$(rv_L)_{t_L} + u_L(rv_L)_r + v_L(rv_L)_\lambda + \dot\theta(rv_L)_\theta = -(\Psi)_\lambda - rfu + F^\lambda - r(v_c)_{t_L} \quad \text{(A1)}$$

$$\begin{aligned}(r\overline{\sigma}\,\overline{v}_L)_{t_L} + r^{-1}(r^2(\overline{\sigma u_L})\overline{v}_L)_r + (r(\overline{\sigma\dot\theta})\overline{v}_L)_\theta + (r\overline{\sigma u_L})\overline{f} \\ = \nabla\cdot\mathbf{F}_L - (r(\overline{\sigma\dot\theta)'v_L'})_\theta - (r\overline{\sigma' v_L'})_{t_L} - r\overline{(\sigma u_L)' f'} \\ - r(\overline{\sigma u_c f}) + r\overline{\sigma F^\lambda} - r\overline{\sigma'(v_c)}_{t_L} \\ = -\frac{r\overline{\sigma}^2}{g}\langle u_L^* \Pi_L^*\rangle - r\overline{\sigma}(\overline{\dot\theta^*(v_L)_\theta}) - r\overline{\sigma}(\overline{u_c f'}) \\ + r\overline{\sigma}\,\overline{F^\lambda}. \end{aligned} \quad \text{(A2)}$$

REFERENCES

Bosart, L. F., and J. A. Bartlo, 1991: Tropical storm formation in a baroclinic environment. *Mon. Wea. Rev.*, **119,** 1979–2013.

——, and G. M. Lackmann, 1995: Postlandfall tropical cyclone reintensification in a weakly baroclinic environment: A case study of Hurricane David (September 1979). *Mon. Wea. Rev.*, **123,** 3268–3291.

Davidson, N. E., G. J. Holland, J. L. McBride, and T. D. Keenan, 1990: On the formation of AMEX tropical cyclones Irma and Jason. *Mon. Wea. Rev.*, **118,** 1981–2000.

DeMaria, M., 1996: The effect of vertical shear on tropical cyclone intensity change. *J. Atmos. Sci.*, **53,** 2076–2087.

——, and J. Kaplan, 1994: A statistical hurricane intensity prediction scheme (SHIPS) for the Atlantic Basin. *Wea. Forecasting,* **9,** 209–220.

——, J.-J. Baik, and J. Kaplan, 1993: Upper level eddy angular momentum fluxes and tropical cyclone intensity change. *J. Atmos. Sci.*, **50,** 1133–1147.

Edmon, H. J., B. J. Hoskins, and M. E. McIntyre, 1980: Eliassen–Palm cross sections for the troposphere. *J. Atmos. Sci.*, **37,** 2600–2616; Corrigendum, **38,** 1115.

Emanuel, K. A., 1986: An air-sea interaction theory for tropical cyclones. Part I: Steady-state maintenance. *J. Atmos. Sci.*, **43,** 585–604.

——, 1997: Some aspects of hurricane inner-core dynamics and energetics. *J. Atmos. Sci.*, **54,** 1014–1026.

Gray, W. M., 1968: Global view of the origin of tropical disturbances and storms. *Mon. Wea. Rev.*, **96,** 669–700.

Guinn, T. A., and W. H. Schubert, 1993: Hurricane spiral bands. *J. Atmos. Sci.*, **50,** 3380–3403.

Holland, G. J., 1987: Mature structure and structure change. *A Global View of Tropical Cyclones*, R. L. Elsberry, Ed., Naval Postgraduate School, 13–52.

——, and R. T. Merrill, 1984: On the dynamics of tropical cyclone structural changes. *Quart. J. Roy. Meteor. Soc.*, **110,** 723–745.

Hoskins, B. J., 1990: Theory of extratropical cyclones. *Extratropical Cyclones: The Erik Palmén Memorial Volume*, C. Newton and E. O. Holopainen, Eds., Amer. Meteor. Soc., 64–80.

——, M. E. McIntyre, and A. W. Robertson, 1985: On the use and significance of isentropic potential vorticity maps. *Quart. J. Roy. Meteor. Soc.*, **111,** 877–946.

Jones, S. C., 1995: The evolution of vortices in vertical shear. Part I: Initially barotropic vortices. *Quart. J. Roy. Meteor. Soc.*, **121,** 821–852.

Lewis, B. M., and D. P. Jorgensen, 1978: Study of the dissipation of Hurricane Gertrude (1974). *Mon. Wea. Rev.*, **106,** 1288–1306.

Marks, F. D., 1985: Evolution of the structure of precipitation in Hurricane Allen (1980). *Mon. Wea. Rev.*, **113,** 909–930.

McBride, J. L., and R. Zehr, 1981: Observational analysis of tropical cyclone formation. Part II: Comparison of non-developing versus developing systems. *J. Atmos. Sci.*, **38,** 1132–1151.

McIntyre, M. E., 1993: Isentropic distributions of potential vorticity and their relevance to tropical cyclone dynamics. *Tropical Cyclone Disasters*, J. Lighthill, G. Holland, Z. Zhemin, and K. Emanuel, Eds., Peking University Press, 143–156.

Miller, B. I., 1958: On the maximum intensity of hurricanes. *J. Meteor.*, **15,** 184–195.

Möller, J. D., and R. K. Smith, 1994: The development of potential vorticity in a hurricane-like vortex. *Quart. J. Roy. Meteor. Soc.*, **120,** 1255–1266.

Molinari, J., 1993: Environmental controls on eye wall cycles and intensity change in Hurricane Allen (1980). *Tropical Cyclone Disasters*, J. Lighthill, G. Holland, Z. Zhemin, and K. Emanuel, Eds., Peking University Press, 328–337.

——, and D. Vollaro, 1989: External influences on hurricane intensity. Part I: Outflow layer eddy angular momentum fluxes. *J. Atmos. Sci.*, **46,** 1093–1105.

——, and ——, 1990: External influences on hurricane intensity. Part II: Vertical structure and response of the hurricane vortex. *J. Atmos. Sci.*, **47,** 1902–1918.

——, ——, and F. Robasky, 1992: Use of ECMWF operational analyses for studies of the tropical cyclone environment. *Meteor. Atmos. Phys.*, **47,** 127–144.

——, S. Skubis, and D. Vollaro, 1995: External influences on hur-

ricane intensity. Part III: Potential vorticity evolution. *J. Atmos. Sci.,* **52,** 3593–3606.
Montgomery, M. T., and B. F. Farrell, 1993: Tropical cyclone formation. *J. Atmos. Sci.,* **50,** 285–310.
——, and R. J. Kallenbach, 1997: A theory for vortex Rossby-waves and its application to spiral bands and intensity changes in hurricanes. *Quart. J. Roy. Meteor. Soc.,* **123,** 435–466.
Ooyama, K. V., 1982: Conceptual evolution of the theory and modeling of the tropical cyclone. *J. Meteor. Soc. Japan,* **60,** 369–379.
Pfeffer, R. L., and M. Challa, 1981: A numerical study of the role of eddy fluxes of momentum in the development of Atlantic hurricanes. *J. Atmos. Sci.,* **38,** 2393–2398.
——, and ——, 1992: The role of asymmetries in Atlantic hurricane formation. *J. Atmos. Sci.,* **49,** 1051–1059.
Plumb, R. A., 1983: A new look at the energy cycle. *J. Atmos. Sci.,* **40,** 1669–1688.
Polvani, L. M., 1991: Two-layer geostrophic vortex dynamics. Part 2. Alignment and two-layer V states. *J. Fluid Mech.,* **225,** 241–270.
Raymond, D. J., 1992: Nonlinear balance and potential vorticity thinking at large Rossby number. *Quart. J. Roy. Meteor. Soc.,* **118,** 987–1016.
Reynolds, R. W., and T. M. Smith, 1994: Improved global sea surface temperature analyses using optimum interpolation. *J. Climate,* **7,** 929–948.
Riehl, H., 1979: *Climate and Weather in the Tropics.* Academic Press, 611 pp.
Rodgers, E. B., J. Stout, J. Steranka, and J. J. Shi, 1991: Satellite observations of variations in tropical cyclone convection caused by upper-tropospheric troughs. *J. Appl. Meteor.,* **30,** 1163–1184.
Rotunno, R., and K. A. Emanuel, 1987: An air–sea interaction theory for tropical cyclones. Part II: Evolutionary study using a nonhydrostatic axisymmetric numerical model. *J. Atmos. Sci.,* **44,** 542–561.
Sadler, J. C., 1976: A role of the tropical upper tropospheric trough in early season typhoon development. *Mon. Wea. Rev.,* **104,** 1266–1278.
Schubert, W. H., 1985: Wave, mean-flow interactions and hurricane development. Preprints, *16th Conf. on Hurricanes and Tropical Meteorology,* Houston, TX, Amer. Meteor. Soc., 140–141.
——, and B. T. Alworth, 1987: Evolution of potential vorticity in tropical cyclones. *Quart. J. Roy. Meteor. Soc.,* **113,** 147–162.
Shapiro, L. J., 1992: Hurricane vortex motion and evolution in a three-layer model. *J. Atmos. Sci.,* **49,** 140–153.
Simpson, R. H., 1971: The decision process in hurricane forecasting. NOAA Tech. Memo. NWS SR-53, 35 pp.
Smith, R. K., 1997: On the theory of CISK. *Quart. J. Roy. Meteor. Soc.,* **123,** 407–418.
Thorncroft, C. D., B. J. Hoskins, and M. E. McIntyre, 1993: Two paradigms of baroclinic-wave life-cycle behaviour. *Quart. J. Roy. Meteor. Soc.,* **119,** 17–55.
Thorpe, A. J., 1985: Diagnosis of balanced vortex structure using potential vorticity. *J. Atmos. Sci.,* **42,** 397–406.
——, 1986: Synoptic-scale disturbances with circular symmetry. *Mon. Wea. Rev.,* **114,** 1384–1389.
Tung, K. K., 1986: Nongeostrophic theory of zonally averaged circulation. Part I: Formulation. *J. Atmos. Sci.,* **43,** 2600–2618.
Willoughby, H. E., 1978: The vertical structure of hurricane rainbands and their interaction with the mean vortex. *J. Atmos. Sci.,* **35,** 849–858.
——, 1990: Temporal changes in the primary circulation in tropical cyclones. *J. Atmos. Sci.,* **47,** 242–264.
——, J. A. Clos, and M. G. Shoreibah, 1982: Concentric eye walls, secondary wind maxima, and the evolution of a hurricane vortex. *J. Atmos. Sci.,* **39,** 395–411.
Wu, C.-C., and K. A. Emanuel, 1993: Interaction of a baroclinic vortex with background shear: Application to hurricane movement. *J. Atmos. Sci.,* **50,** 62–76.